Colloid Polym Sci (2008) 286:489–498
DOI 10.1007/s00396-007-1824-4

INVITED REVIEW

Photopolymerization of water-soluble acrylic monomers induced by colloidal CdS and $Cd_xZn_{1-x}S$ nanoparticles

Alexander L. Stroyuk · Ivan V. Sobran · Anna V. Korzhak · Alexandra E. Raevskaya · Stepan Ya. Kuchmiy

Received: 30 July 2007 / Revised: 18 October 2007 / Accepted: 2 December 2007 / Published online: 8 January 2008

Abstract Photocatalytic activity of CdS and $Cd_xZn_{1-x}S$ nanoparticles in the polymerization of acrylamide and acrylic acid in aqueous solutions has been found. It has been shown that the most probable way of the photogeneration of primary radicals is the reduction of an adsorbed monomer by the conduction band electrons of the semiconductor nanoparticles, a monomer oxidation by the valence band holes and atomic hydrogen addition to a monomer being complementary photoinitiation routes. A correlation between the composition of $Cd_xZn_{1-x}S$ nanoparticles and their photocatalytic activity in the acrylamide polymerization has been established. It has been shown that an increase in the quantum yield of the photopolymerization in a sequence $CdS < Cd_{0.75}Zn_{0.25}S < CdS_{0.5}Zn_{0.5}S < Cd_{0.3}Zn_{0.7}S$ originates from a concurrent increase of the conduction band potential of the semiconductor nanoparticles. A kinetic equation of the photocatalytic acrylamide polymerization has been derived. Quantum yields of the photoinitiation have been found to be as small as 10^{-4} to 10^{-3}.

Keywords Semiconductor nanoparticles · Cadmium sulfide · Zinc sulfide · Photocatalysis · Photopolymerization · Acrylic acid · Acrylamide

A. L. Stroyuk (✉) · I. V. Sobran · A. V. Korzhak · A. E. Raevskaya · S. Y. Kuchmiy
Pysarzhevski Institute of Physical Chemistry,
National Academy of Sciences of Ukraine,
31 Nauky av.,
03028 Kyiv, Ukraine
e-mail: stroyuk@inphyschem-nas.kiev.ua

Introduction

A particular feature of $Cd_xZn_{1-x}S$ solid solutions consists in a substantial increase in the conduction band potential (from −0.8 V vs normal hydrogen electrode (NHE) for CdS [1, 2] to −1.8 V for ZnS [3, 4]) accompanied by a comparatively small increment in the valence band potential (from 1.6 V for CdS [1, 2] to 1.8 V for ZnS [3, 4]) as x varies from unity to zero. It is known that cadmium and zinc sulfides as well as mixed $Cd_xZn_{1-x}S$ compounds can all be used as photocatalysts in a number of redox processes, in particular, molecular hydrogen evolution [3, 5, 6]. The efficiency of photocatalytic processes depends on the overvoltage—the gap between the conduction (valence) band of a semiconductor and the reduction (oxidation) potential of a substrate. From this viewpoint, mixed $Cd_xZn_{1-x}S$ semiconductors can serve as a convenient "toolkit" for the investigation of the energetics of reductive photocatalytic reactions, since their conduction band potential could be tuned in a wide range via a variation in the composition of a photocatalyst.

Among the photocatalytic reactions proceeding with the participation of semiconductor crystals, an important place belongs to the photopolymerization [7–16]. This is due to several reasons. First, the investigation of the characteristic features of the photopolymerization initiated on the surface of a semiconductor often reveals subtle effects associated with the structure or surface imperfection of the crystal. The most minuscule changes in the ability of the semiconductor crystal to initiate chain-radical processes caused by a change of either its size or the surface structure multiply thousands-fold as the polymeric chain propagates and so can be noticed at the analysis of the polymerization kinetics and polymer properties. Second, in contrast to many other photocatalytic reactions investigated mostly in the model

systems, the photopolymerization induced by semiconductor crystals and, especially, nanometer particles (NPs) [7, 8, 10], homogeneously dispersed both in starting mixture and in a polymeric product, can be directly used for the development of new photocurable compositions and functional polymer materials.

Many technologies built on photopolymerization systems, such as lithography, stereolithography, holography, etc., put specific demands on the properties of the photoinitiators (for example, sensitivity to the visible light and water solubility), monomers used and polymers obtained (specific combination of solubility and hardness of a polymer, low shrinkage and insensitivity to oxygen, etc.) [17–19], which could hardly be met with traditional organic photoinitiators. In this view, utilization of semiconductor NPs as photoinitiators opens new possibilities for the development of these technologies.

In the present work, the photocatalytic activity of CdS and $Cd_xZn_{1-x}S$ NPs in acrylic acid (AAc) and acrylamide (AAm) polymerization in aqueous solutions is studied. These NPs are shown to be efficient photoinitiators of chain-radical polymerization processes, demonstrating a unique combination of the sensitivity to the visible light with the indifference to the presence of molecular oxygen. The work is accented on the discussion of primary initiation steps of the photopolymerization, a correlation between the photopolymerization rate and the composition of $Cd_xZn_{1-x}S$ NPs as well as the kinetics and mechanism of the photocatalytic polymerization.

Experimental

Reagents and NPs synthesis $CdCl_2$, $ZnCl_2$, sodium polyphosphate (SPP), Na_2S, acrylamide, acrylic acid, methylviologen (MV^{2+}) chloride, Na_2SO_3, $KBrO_3$, KBr, and KI were purchased from Aldrich and used without additional purification. $Cd_xZn_{1-x}S$ NPs (where $x=[CdCl_2]_0\times([CdCl_2]_0+[ZnCl_2]_0)^{-1}$) were prepared mixing sodium sulfide with cadmium(II) and zinc(II) chlorides in aqueous SPP solutions. The details of the preparation and characterization of $Cd_xZn_{1-x}S$ NPs can be found elsewhere [20].

Instrumental Absorption spectra of solutions were taken on a Specord 210 double beam spectrophotometer. Flash photolysis experiments were performed according to [21, 22] with the home-made setup. The optical density of the nonstationary absorbance (ΔD_0) was scanned in 400–700 nm spectral window with the precision ±0.003 after complete decay of the excitatory light impulse (40 μs). Stationary irradiation of solutions was performed in quartz 1.0 cm parallel-side cuvettes with a mercury high pressure 1,000 W lamp. The light was filtered to give a narrow spectral band with $\lambda_{max}=365$ nm or the visible band with $\lambda>400$ nm. In some experiments, solutions were degassed before the irradiation. Light source intensity was varied by means of the calibrated metal grids. The data presented in the figures were obtained at $I_0=2.34\times10^{-7}$ Einstein/s if not stated otherwise in the caption.

Monomer concentration determination Monomer concentration was measured via double bond bromination by a mixture of sodium bromide and bromate followed by the iodometric determination of residual bromine. In typical procedure, 0.2 ml aliquot of a tested solution was added to 8.0 ml of a solution containing 0.50 M H_2SO_4 and 0.11 M KBr followed by the 0.8 ml 0.05 M $KBrO_3$ solution. The mixture was kept in dark at room temperature for 10–15 min to let the bromination finish. Then, 1.0 ml potassium iodide 2.0 M solution was added to the mixture. In 5 min, 0.1 ml aliquot was taken from the mixture and introduced into 9.9 ml KI 2.0 M solution. The optical density of the resulting KI_3 solutions at 351 nm was measured and used for the calculation of the monomer concentration.

Calculations Initial rate of the photopolymerization R_p was calculated as a decrement of the monomer concentration in the first 10–15 min of the irradiation. Quantum yield of the photopolymerization Φ was determined as $\Phi=R_p\nu_{cuv}\cdot(1{,}000\cdot I)^{-1}$, where ν_{cuv} is the solution volume (2 ml), I is the intensity of the de facto absorbed light. The viscosity-average molecular mass of polymeric products was determined using an Ostwald capillary viscosimeter. The band gap of $Cd_xZn_{1-x}S$ NPs (E_g) was calculated as an energy corresponding to the intersection point between the abscissae axis and a tangent to the edge of the absorption band of a colloidal solution (λ_{tr}) as $E_g=1{,}240/\lambda_{tr}$ [2].

Results and discussion

Structural, optical, and photochemical properties of $Cd_xZn_{1-x}S$ NPs The reaction between a mixture of cadmium and zinc chlorides and sodium sulfide in aqueous SPP solutions results in the formation of stable colloidal $Cd_xZn_{1-x}S$ solutions provided the precursor concentrations do not exceed 1×10^{-2} M. At small concentrations, $1–5\times10^{-4}$ M, the Cd:Zn ratio in $Cd_xZn_{1-x}S$ NPs can somewhat deviate from those in the initial solution [20] due to faster precipitation of CdS as compared with ZnS and partial binding of Zn^{II} in complexes with OH^-, water, and other species. In this connection, more concentrated sols ($5\times10^{-3}–1\times10^{-2}$ M) were used in the present work, where Cd:Zn ratio is the same both in the starting Cd^{II} and

Zn^{II} chlorides solution and in the colloidal $Cd_xZn_{1-x}S$ NPs. Figure 1a represents XRD spectra of the coagulates collected from the solutions with $[Cd_xZn_{1-x}S]=[SPP]=5\times10^{-3}$ M. The spectra are composed of the three diffuse peaks indicating the presence of ultra-small particles with cubic zinc blende crystalline motive. The size of $Cd_xZn_{1-x}S$ NPs calculated using the Scherer formula was found to be 6.0±0.5 nm independently of the NPs composition. Interplanar distances in $Cd_xZn_{1-x}S$ NPs change with x according to the Vegard law (Fig. 1b) indicating $Cd_xZn_{1-x}S$ NPs be homogeneous solid solutions.

The position of the absorption threshold (λ_{tr}) of colloidal SPP-stabilized $Cd_xZn_{1-x}S$ NPs was found to depend on x and the concentrations of both the reagents and the stabilizer. At $[Cd_xZn_{1-x}S]=[SPP]=5\times10^{-3}$ M, the variation of x from 0 to 1.0 results in the λ_{tr} shift from 330–335 (Fig. 2, curve 1) to 510–515 nm (Fig. 2, curve 5) corresponding to the decrease of the band gap E_g from 3.70−3.75 to 2.41−2.43 eV.

Stationary irradiation of air-exposed CdS and $Cd_xZn_{1-x}S$ colloids results in a gradual decrease in the optical density of solutions due to oxidative photocorrosion of semiconductor NPs [1, 7]. For CdS, this process can be described by the following brutto reaction:

$$CdS + 2O_2 \xrightarrow{h\nu} Cd^{2+} + SO_4^{2-} \quad (1)$$

The oxidative photocorrosion of $Cd_xZn_{1-x}S$ and CdS NPs also takes place in the presence of the both monomers, the reaction rate being greater in the case of AAc (Fig. 3) due to the photocorrosion acceleration in acidic media [1, 23].

Light absorption by $Cd_xZn_{1-x}S$ NPs results in the semiconductor excitation and subsequent generation of conduction band electrons (e^-_{CB}) and valence band holes (h^+_{VB}) both on the surface and in the volume of NPs. Free charge carriers are rapidly trapped by localized surface states (lattice defects, noncompensated surface atoms, etc. [24–26]) or decay via nonradiative recombination pathways. The valence band hole trapping by surface S^{2-} ions results in the formation of $S^{\bullet-}$ anion radicals:

$$h\nu + Cd_xZn_{1-x}S \rightarrow Cd_xZn_{1-x}S\left(e^-_{CB} + h^+_{VB}\right) \quad (2)$$

$$e^-_{CB} + [\,]_e \rightarrow e^-_{tr} \quad (3)$$

$$h^+_{VB} + [\,]_h \rightarrow h^+_{tr}(\text{or } S^{\bullet-}) \quad (4)$$

where $[]_e$ and $[]_h$ are electron and hole traps, e^-_{tr} and h^+_{tr} are trapped electron and hole.

Trapped charge carriers can recombine with free opposite charges emitting "defect" luminescence h_{lum} (process 5) or react with adsorbed species.

$$e^-_{CB}\left(e^-_{tr}\right) + h^+_{tr}\left(h^+_{VB}\right) \rightarrow h\nu_{lum} \quad (5)$$

Sodium sulfite has affinity to the surface of colloidal cadmium and zinc sulfides and can act as a very efficient valence band hole scavenger (reaction 6), capable of suppressing the most of recombination pathways.

$$h^+_{VB,tr} + SO_3^{2-}\left(HSO_3^-\right) \rightarrow SO_3^{\bullet-}\left(HSO_3^{\bullet}\right) \quad (6)$$

At the illumination of Na_2SO_3-containing CdS colloids with short powerful light flashes, the generation of many electron-hole couples per semiconductor NP takes place. As the holes are captured in the reaction 6 nanocrystals become negatively charged by the electrons survived in the recombination processes due to the surface trapping.

The negative charge accumulation by CdS NPs results in an optical band gap increase and a reversible hypsochromic shift of the NPs absorption threshold (so called dynamic Burstein–Moss effect) [27–29]. This transient shift is observed as a nonstationary bleaching band in the differential absorption spectra of CdS NPs, its intensity being proportional to the density of negative charge. The scavenging of e^-_{tr} by dissolved oxygen (reaction 7) results in the decay of

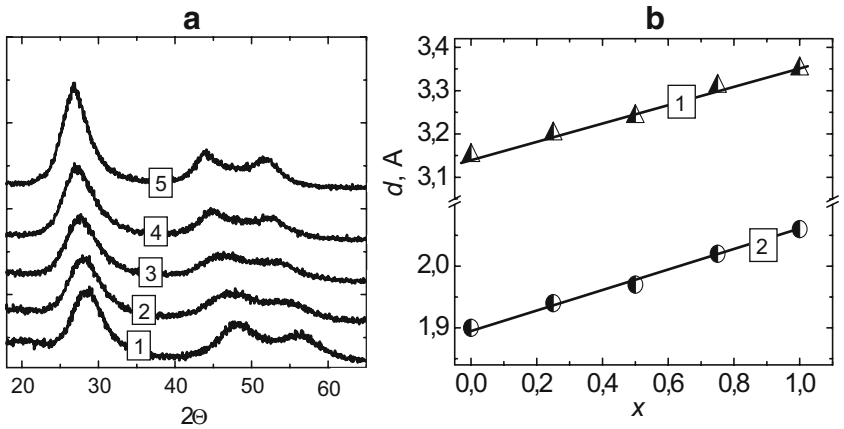

Fig. 1 **a** XRD spectra of $Cd_xZn_{1-x}S$ NPs at x=0 (*1*), 0.25 (*2*), 0.5 (*3*), 0.75 (*4*), and 1.0 (*5*); **b** interplanar distances d_{111} (*1*) and d_{220} (*2*) as a function of the $Cd_xZn_{1-x}S$ NPs composition

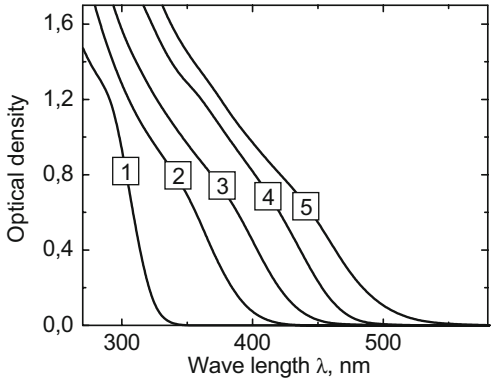

Fig. 2 Absorption spectra of the SPP-stabilized colloidal $Cd_xZn_{1-x}S$ solutions at x=0 (*1*), 0.25 (*2*), 0.50 (*3*), 0.75 (*4*), and 1.00 (*5*). $[Cd_xZn_{1-x}S]_0$=[SPP]=5×10^{-3} M, cuvette l=0.2 cm

nonstationary bleaching over a period of tens-hundreds of microseconds.

$$e_{tr}^- + O_2 \rightarrow O_2^{\bullet -} \quad (7)$$

Electron acceptors, capable of strong adsorption on the surface of CdS NPs, for example, methylviologen MV^{2+}, can scavenge the photogenerated electron (process 8) even before the surface trapping occurs.

$$e_{CB}^- + MV^{2+} \rightarrow MV^{\bullet +} \quad (8)$$

This results in almost total suppression of all other primary photophysical and photochemical processes involving the conduction band electrons [1, 27, 30]. Thus, no nonstationary bleaching signals are observed in the presence of even trace amounts of methylviologen (~10^{-7} M). So, the affinity of various chemical species to the surface of CdS NPs as well as their reactivity towards the photogenerated charge carriers can be probed using the kinetic spectrophotometry under flash photoexcitation.

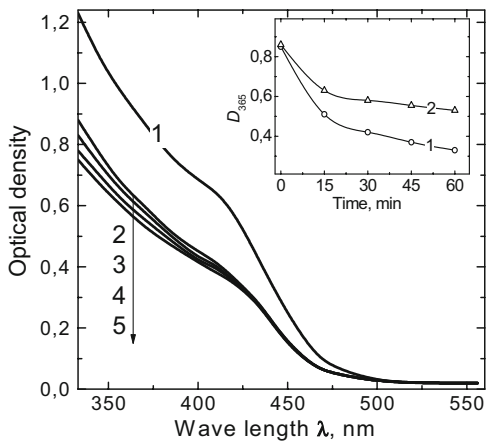

Fig. 3 Evolution of the absorption spectrum of the air-exposed colloidal CdS solution with [CdS]=1×10^{-3} M, [SPP]=3×10^{-3} M, [AAc]=0.5 M before (*curve 1*) and after the irradiation for 15 (*2*), 30 (*3*), 45 (*4*), and 60 min (*5*), l=1.0 cm. *On the inset* Decrease of the optical density of CdS colloid at 365 nm (D_{365}) as a function of the irradiation duration for the AAc (*curve 1*) and AAm (*curve 2*). $[AAc]_0=[AAm]_0$=0.5 M

It has been found that the AAc affects non-stationary bleaching band of CdS NPs similarly to methylviologen, decreasing the intensity of the transient signal. The decrement is proportional to the concentration of the monomer (Fig. 4a) implying that AAc participates in the scavenging of the photogenerated conduction band electrons (reaction 9).

$$e_{CB}^- + M \rightarrow M^{\bullet -} \quad (9)$$

Quite a substantial AAc concentration (0.15–0.20 M) is necessary to halve the intensity of the nonstationary bleaching band, the fact indicating weak adsorption of the monomer on the surface of CdS NPs. Given in Fig. 4a, dependence between the transient signal intensity and the AAc concentration can therefore be approximated by a Langmuir Eq. 10.

$$\frac{\Delta D_0 - \Delta D_{AAc}}{\Delta D_0} = k_{AAc}\theta_{AAc} = k_{AAc}\frac{K[AAc]}{1+K[AAc]} \quad (10)$$

where K is an AAc adsorption constant, ΔD_0 and ΔD_{AAc} are the intensities of the transient signal before and after the addition of the monomer.

From the Eq. 10 one obtains

$$\frac{\Delta D_0}{\Delta D_0 - \Delta D_{AAc}} = \frac{1}{k_{AAc}} + \frac{1}{k_{AAc}K[AAc]} \quad (11)$$

In accordance with the expression 11, a linear correlation between $\Delta D_0\times(\Delta D_0-\Delta D_{AAc})^{-1}$ and $[AAc]^{-1}$ is actually observed (Fig. 4b).

General characterization of the AAc and AAm photopolymerization in the presence of CdS and $Cd_xZn_{1-x}S$ NPs Complete and equivalent light absorption by $Cd_xZn_{1-x}S$ NPs throughout the entire range of x values can be achieved only if the solutions are illuminated by a short-wave source, for example, with the mercury 253.9 nm line. However, noncatalytic spontaneous photopolymerization of both the AAc and AAm was found to take place under such irradiation. So, to avoid possible interference of the noncatalytic and photocatalytic processes, longer-wave mercury line with λ=365 nm was usually used to excite $Cd_xZn_{1-x}S$ NPs. In this connection the range of the photocatalysts tested was restricted to $x\geq0.3$.

When there is no photocatalyst present in a monomer solution (0.5–10.0 M), its concentration remains constant at prolonged (3–4 h) illumination. In the presence of CdS or $Cd_xZn_{1-x}S$ NPs, fast reduction of the monomer concentration and growth of the solution viscosity due to polymer formation are observed. The facts indicate that the photocatalytic polymerization takes place with the participation of semiconductor NPs. Figure 5a demonstrates kinetic

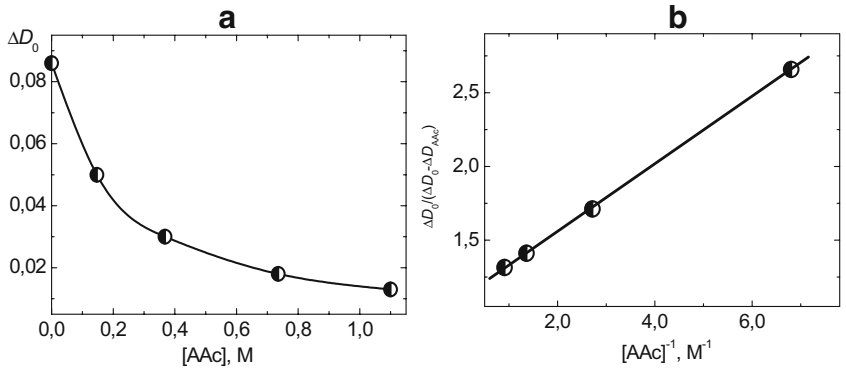

Fig. 4 **a** The intensity of CdS NPs nonstationary bleaching band (ΔD_0) at 480 nm vs the AAc concentration. [CdS]=1×10^{-3} M, [SPP]=3×10^{-3} M, [Na_2SO_3]=1×10^{-2} M. **b** A dependence $\Delta D_0/(\Delta D_0-\Delta D_{AAc})$ vs $[AAc]^{-1}$ for the data presented in Fig. 3a

curves of the AAm photopolymerization in solutions of various composition. It can be seen from the comparison of curves 1 and 2 in Fig. 5a that about half the monomer is converted into the polyacrylamide in the first 10–15 min of the illumination with 70–80% monomer conversion after 1 h irradiation. A gradual drop of the photopolymerization rate can be accounted for by the monomer consumption and NPs surface blocking by the polymer.

Both the conduction band electrons and the valence band holes can in principle initiate the photopolymerization via, respectively, reduction or oxidation of a monomer to ion radicals. The former of these processes was directly shown to take place at the flash photolysis of AAc-containing CdS colloids. In case of $Cd_xZn_{1-x}S$ NPs these processes are expected to proceed more efficiently since, as will be shown below, an increment of the molar Zn(II) fraction in $Cd_xZn_{1-x}S$ NPs results in a large increase in the conduction band potential. At the same time, the valence band potentials of both CdS and $Cd_xZn_{1-x}S$ NPs are sufficiently high for the monomers oxidation ($E_{VB}\geq1.6$ V vs NHE).

A relative contribution of the conduction band electrons and valence band holes into the photoinitiation of the polymerization can be separately estimated with the help of agents capable of selective scavenging of one sort of the charge carriers. In such a way, a relative contribution of e^-_{CB} can be deduced studying the photopolymerization in the presence of sodium sulfite, which can scavenge h^+_{VB} and suppress the monomers oxidation. On the other hand, carrying out the photopolymerization in the presence of MV^{2+} one can eliminate a contribution of the monomer reduction by e^-_{CB}.

Comparison of the curves 1 and 4 or 2 and 5 in Fig. 5a shows that the photopolymerization rate falls by a factor of four—from 2.75×10^{-4} to 0.7×10^{-4} M/s in the case of CdS NPs and from 3.83×10^{-4} to 0.92×10^{-4} M/s in the case of $Cd_{0.5}Zn_{0.5}S$ NPs, when the photoreaction is carried out in the presence of methylviologen. It should be noted that the photopolymerization rate does not fall to zero, although the MV^{2+} concentration is three orders higher than that sufficient for complete scavenging of the photogenerated electrons. The fact speaks in favor of the h^+_{VB} participation in the photopolymerization, the relative contribution of this channel of primary radical generation not exceeding 25%. The conclusion about the dominating role of e^-_{CB} in the photoinitiation is also supported by a 60% increase in the AAc photopolymerization rate, from 2.75×10^{-4} to $4.47\times$

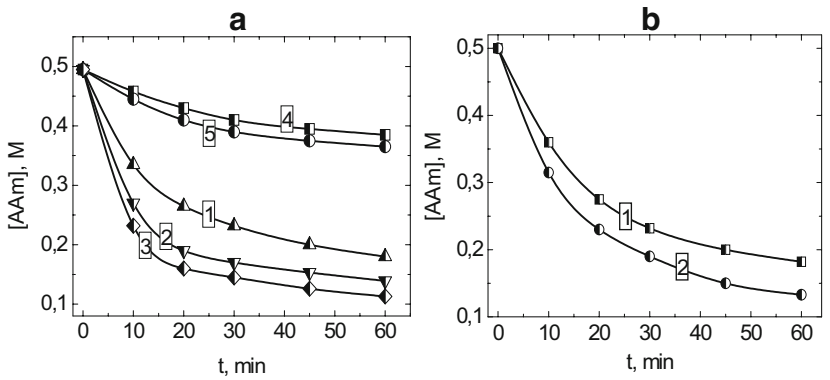

Fig. 5 **a** Kinetic curves of the AAm photopolymerization in degassed solutions in the presence of CdS (*1*) and $Cd_{0.5}Zn_{0.5}S$ NPs (*2*) only, CdS NPs and Na_2SO_3 (*3*), CdS NPs and MV^{2+} (*4*), and $Cd_{0.5}Zn_{0.5}S$ NPs and MV^{2+} (*5*). **b** Kinetic curves of the AAm photopolymerization in the presence of CdS NPs in air-exposed (*curve 1*) and degassed solutions (*curve 2*). [$Cd_xZn_{1-x}S$]=1×10^{-3} M, [SPP]=3×10^{-3} M, [AAm]=0.5 M, [Na_2SO_3]=0.1 M, [MV^{2+}]=1×10^{-3} M

10^{-4} M/s (compare curves 1 and 3 in Fig. 5a) when Na_2SO_3 is introduced into a solution. Sulfite ions, though suppressing complementary photoinitiation route with the participation of h^+_{VB}, impede strongly the recombination processes and promote in this way the monomer reduction by e^-_{CB}.

The rate of AAm photopolymerization in air-exposed solutions is only by a third smaller than that observed in degassed solutions (compare curves 1 and 2 in Fig. 5b). It can therefore be concluded that oxygen does not affect noticeably the primary photochemical events on the surface of semiconductor NPs. This is a striking feature of the semiconductor NPs distinguishing them from organic photoinitiators. The absence of any induction periods during the first 5–10 min of the AAc and AAm photopolymerization in the presence of air indicates that oxygen is a weak inhibitor in the systems under investigation. It is known that during an initial stage of the radical photopolymerization oxygen can build into the growing polymer chain giving regular—$(M–O–O–M–O–O)_n$—structures (where M is a monomer) [31–33]. There is approximately 3×10^{-4} M of the oxygen in air-saturated water at 18–20 °C [34]. Taking into account that typical photopolymerization rates are $(2.0–5.0)\times10^{-4}$ M/s, one can expect sharp decrease in O_2 concentration in the first minutes of the photoreaction, while the diffusion of new portions of oxygen would be hindered due to increased viscosity of a solution and lack of the stirring.

It is widely accepted that the photopolymerization of acrylic monomers in aqueous solutions proceeds only via a free-radical mechanism [31, 33]. This mechanism implies transformation of primary charged monomer radicals (reactions 9 and 13) into neutral radical species. As probable routes for these transformations, the protonation of an anion radical (reaction 12) and the deprotonation of a cation-radical deprotonation (reaction 14) can be accepted [33].

$$M^{\bullet-} + H^+(H_2O) \rightarrow HM^{\bullet}(+OH^-) \quad (12)$$

$$H - M + h^+_{VB} \rightarrow H - M^{+\bullet} \quad (13)$$

$$H - M^{\bullet+} \rightarrow M^{\bullet} + H^+ \quad (14)$$

It is well-known that the $Cd_xZn_{1-x}S$ NPs can be used as an efficient photocatalyst of hydrogen evolution from aqueous solutions [3, 5]. Taking the fact into account, an alternative scheme of primary radicals generation can be proposed. In this scheme, the primary neutral radicals are generated via hydrogen atom addition to a monomer molecule according to the following scheme:

$$e^-_{CB}\left(e^-_{tr}\right) + H_2O \rightarrow H^{\bullet} + OH^- \quad (15)$$

$$H^{\bullet} + M \rightarrow HM^{\bullet} \quad (16)$$

To assess the probability of this photoinitiation route an effect of AAm on the photocatalytic hydrogen evolution from an aqueous solution of sodium sulfite (1×10^{-2} M) and $Cd_{0.5}Zn_{0.5}S$ NPs (5×10^{-3} M) was studied. This process becomes noticeably less efficient already in the presence of small amounts of AAm ($\sim10^{-3}$ M) and is quenched completely at [AAm]=$1\cdot10^{-2}$ M, confirming the validity of the assumption on the possible participation of atomic hydrogen in the generation of primary monomer radicals.

The effect of $Cd_xZn_{1-x}S$ NPs composition on the rate of AAm photopolymerization Figure 6 shows the kinetic curves of the AAm photopolymerization in the presence of $Cd_xZn_{1-x}S$ NPs of various composition. The variation of the quantum yield of the photoprocess with x (Table 1) also supports the assumption about the dominating role of the reaction 9 as a primary radicals source. It can be seen from Table 1 that the quantum yield grows from 3.2 to 5.8 with the molar Cd(II) fraction in $Cd_xZn_{1-x}S$ NPs decreasing from 1.0 to 0.3. Experimental conditions being maintained equivalent one can assume that the increase in the quantum yield of the AAm photopolymerization in a sequence CdS < $Cd_{0.75}Zn_{0.25}S$ < $CdS_{0.5}Zn_{0.5}S$ < $Cd_{0.3}Zn_{0.7}S$ originates from an increase in the rate of primary radicals formation (i.e. reactions 9, 12, 13, and 14).

The valence band potential E_{VB} of the bulk cadmium and zinc sulfides is 1.6 V [1, 2] and 1.8 V [3, 4] vs NHE, respectively. Combining these values with the band gap energies E_g of bulk cubic CdS (2.4 eV) [1, 2] and ZnS (3.6 eV) [3, 4] one obtains the conduction band potentials for cadmium sulfide E_{CB}=−0.8 V and zinc sulfide E_{CB}=−1.8 V. Comparison of both E_{CB} values shows that the conduction

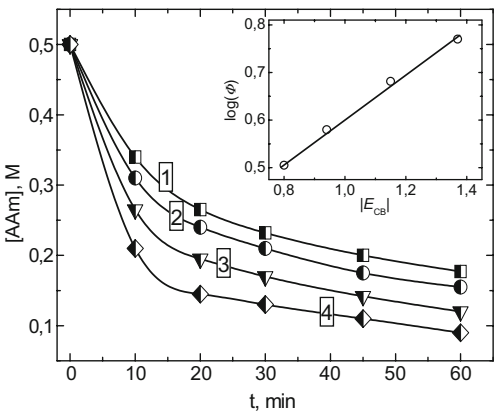

Fig. 6 Kinetic curves of the AAm photopolymerization in air-exposed solutions induced by CdS (*1*), $Cd_{0.75}Zn_{0.25}S$ (*2*), $Cd_{0.5}Zn_{0.5}S$ (*3*), and $Cd_{0.3}Zn_{0.7}S$ NPs (*4*). *On the inset* A semilogarithmic correlation between the quantum yield of AAm photopolymerization and the conduction band potential of $Cd_xZn_{1-x}S$ NPs. [$Cd_xZn_{1-x}S$]=1×10^{-3} M, [SPP]=3×10^{-3} M, [AAm]=0.5 M

Table 1 The initial rate (R_p), total quantum yield (Φ), photoinitiation quantum yield (β) of AAm photopolymerization, and the quantum yield of methylviologen reduction ($\Phi(MV^{\bullet+})$) in the presence of $Cd_xZn_{1-x}S$ NPs

x	Φ	E_{CB}, V	$\beta \cdot 10^3$	$\Phi(MV^{\bullet+})\cdot 10^3$
0.30	5.8	–1.37	1.0	1.5
0.50	4.8	–1.15	0.7	1.3
0.75	3.8	–0.94	0.4	1.1
1.00	3.2	–0.80	0.3	0.6

Quantum yields Φ were determined at $[Cd_xZn_{1-x}S]=1\times10^{-3}$ M, [SPP] = 3×10^{-3} M, [AAm]=0.5 M, MV^{2+} reduction was studied at $[Cd_xZn_{1-x}S]=1\times10^{-3}$ M, [SPP]=3×10^{-3} M, $[Na_2SO_3]=1\times10^{-2}$ M

band increment from CdS to ZnS (1.0 eV) is five times higher than that of the valence band potential (0.2 V). The dependence between the quantum yield of AAm photopolymerization and the composition of $Cd_xZn_{1-x}S$ NPs is therefore likely to originate not from the variation of the valence band energy but from the E_{CB} increase with decreasing x.

A difference between the E_{VB} values of cadmium and zinc sulfides being comparatively small, the utilization of a simple linear combination 17 for the calculation of $E_{VB}(x)$ would not apparently introduce substantial error into the determination of the conduction band potential of nanoparticulate $Cd_xZn_{1-x}S$ from the Eq. 18.

$$E_{VB}(x) = xE_{VB}(CdS) + (1-x)E_{VB}(ZnS) \quad (17)$$

$$E_{CB}(x) = E_{VB}(x) - Eg(x) \quad (18)$$

The E_{CB} values computed by this method for CdS and $Cd_xZn_{1-x}S$ NPs at x=0.3, 0.5 and 0.75 are presented in Table 1. It can be seen from the table that Φ increases along with the augmentation of the conduction band potential of the semiconductor NPs.

Correlations between a rate constant of the interfacial charge transfer k_{et} (which determines the quantum yields of the photoinitiation and the photopolymerization in the whole) and the energies of an electron donor E_D (E_D = $E_{CB}(x)$ in the case under discussion) and an acceptor E_A (here, one-electron AAm reduction potential E_{AAm}) can be described by a Tafel equation [28, 30]:

$$\log\left(k_{et}/k_{et}^0\right) = \alpha\cdot(E_D - E_A) \quad (19)$$

where k_{et}^0 is a charge transfer rate constant at a standard potential, α is a coefficient.

If the observed $\Phi - x$ dependence is actually determined by the overvoltage of the reaction 9, $E_{CB}(x) - E_{AAm}$, a linear dependence between $\log(\Phi)$ and $E_{CB}(x)$ should exist. This was found to be the case (see inset in Fig. 6), supporting the assumption about the crucial role of the rate of the electron transfer from the conduction band of $Cd_xZn_{1-x}S$ NPs to the monomer molecules.

Kinetics of the AAc and AAm photopolymerization in the presence of CdS and $Cd_xZn_{1-x}S$ NPs

1. The initial monomer concentration

Figure 7 illustrates a dependence between the photopolymerization rate of AAc (curve 1) or AAm (curve 2) and the starting concentration of the monomers. Kinetic orders by the monomer concentration, n_M=1.55±0.05 for AAc and n_M=1.45±0.05 for AAm were calculated from the logarithmic transforms of the curves 1 and 2 (see inset in Fig. 7).

A linear dependence between the rate and the initial monomer concentration is usually observed (n_M=1.0) when the chain-radical photopolymerization of acrylic monomers is initiated by molecular photoinitiators [31, 33].

As the most probable reason for the kinetic reaction order by the monomer being greater than unity, the participation of the monomer in the primary radicals generation can be assumed. Indeed, when molecular photoinitiators (for example carbonyl aromatic compounds, polyvalent metal complexes [17, 33], dyes [33–35], etc.) are used to induce photopolymerization, the light absorption results either in a photoinitiator decomposition or its transition into an excited state, which interacts further with components of a solution, in particular, with a solvent, giving primary radicals. At that, the monomer reacts either with primary radicals generated from a photoinitiator or with growing polymer chain, participating exclusively in the chain propagation stage. In the systems under discussion, a monomer oxidation by h_{VB}^+ or its reduction by e_{CB}^- results directly in the monomer radicals formation. Involve-

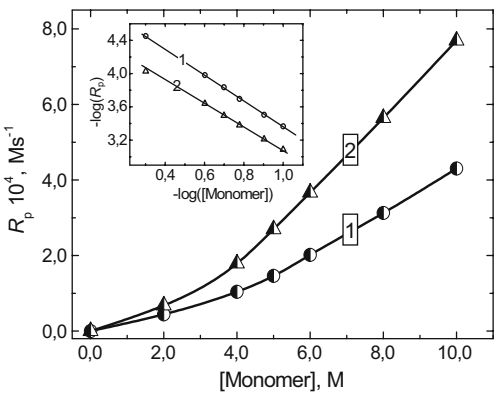

Fig. 7 The rate of AAc (*curve 1*) and AAm (*curve 2*) photopolymerization in the presence of CdS and $Cd_{0.5}Zn_{0.5}S$ NPs, respectively, vs the initial monomer concentration. *On the inset* The same correlations in the logarithmic coordinates. Degassed solutions, $[Cd_xZn_{1-x}S]=1\times10^{-3}$ M, [SPP] = 3×10^{-3} M, $I_0=1.67\times10^{-7}$ Einstein/s

ment of the monomers both into the photoinitiation and chain propagation can result in an increase of n_M up to 1.5. Not only the photopolymerization rate but also the molecular mass of polymeric products depends upon the initial monomer concentration. In air-exposed $Cd_{0.5}Zn_{0.5}S$ NPs (1×10^{-3} M) and AAm solutions, the molecular mass of polyacrylamide is 0.2×10^6 g/mole at $[AAm]_0=0.5$ M, $(0.45–0.50)\times10^6$ g/mole at $[AAm]_0=0.75$ M, and $(1.25–1.30)\times10^6$ g/mole at $[AAm]_0=1.0$ M.

2. The irradiation intensity

Relations between I_0 and the photopolymerization rate of both AAc (Fig. 8a, curve 1) and AAm (Fig. 8a, curve 2) are described by power dependences typical for the free-radical photopolymerization of acrylic monomers [31, 33]. The kinetic polymerization orders by the light intensity can be obtained: $n_I=0.37\pm0.02$ for AAc and $n_I=0.33\pm0.02$ in case of AAm (Fig. 8b). These parameters are lower than $n_I=0.5$—the value typical for the photoinduced polymerization with the macroradicals recombination as basic termination way [31, 33]. The fact is probably due to a nonlinear growth of the efficiency of the recombination processes in $Cd_xZn_{1-x}S$ NPs with the light intensity increment [30, 36, 37]. This supposition is confirmed further by a decrease of the quantum yield Φ, both at the AAc photopolymerization in degassed solutions (Table 2) and the AAm polymerization in the presence of oxygen (Table 3), with an increase in I_0.

3. The NPs concentration

A dependence between the initial rate of the AAm photopolymerization and the molar $Cd_{0.5}Zn_{0.5}S$ concentration is given in Fig. 9 both for degassed (curve 1) and aerated (curve 2) solutions. The plateau on the curve 1 at $[Cd_{0.5}Zn_{0.5}S]>8\cdot10^{-4}$ M can be the result of the saturation of the light absorption. A difference in the form of the curves 1 and 2 is probably due to the fact that at low NPs contents, when the light absorption and consequent primary radicals concentration is small, the oxygen consumption is slow allowing effective quenching of the macrochains growth.

The equation of the photopolymerization rate The kinetic relations discussed above are typical for the chain-radical AAc and AAM polymerization as expected. The primary monomer radicals, which are supposed to be generated in the reactions 9, 12, 13, and 14 and, to some extent, in the process 16, participate further in the propagation of chains:

$$M^\bullet + M \rightarrow M_2^\bullet + M \rightarrow \ldots \rightarrow M_n^\bullet \quad (20)$$

The chain termination occurs mainly at the recombination of the two growing macroradicals [31, 33] as indicated by the kinetic orders by the light intensity:

$$2M_n^\bullet \rightarrow P_{2n} \quad (21)$$

where P_{2n} is a nonactive polymeric product. The rate expressions for the photochemical chain initiation (R_{in}), propagation (R_p), and termination (R_t) can be expressed as follows

$$R_{in} = \beta[M]I \quad (22)$$

$$R_p = k_p[M][M^\bullet] \quad (23)$$

$$R_t = k_t[M^\bullet]^2 \quad (24)$$

where β is the quantum yield of the photoinitiation, I is the absorbed light intensity, k_p and k_t are constants of the chain propagation and termination.

Applying the stationarity condition ($R_{in}=R_t$) to the expressions 22 and 24 and assuming that R_p does not alter with the chain length [31, 33] one obtains

$$[M^\bullet] = (\beta/k_t)^{0.5}[M]^{0.5}I^{0.5} \quad (25)$$

The equations for the R_p can be then composed from expressions 23 and 25:

$$Rp = \left(kp/k_t^{0.5}\right)\beta^{0.5}[M]^{1.5}I^{0.5} \quad (26)$$

The exponents at the monomer concentration (1.5) and the light intensity (0.5) in the expression 26 agree well with the experimental values.

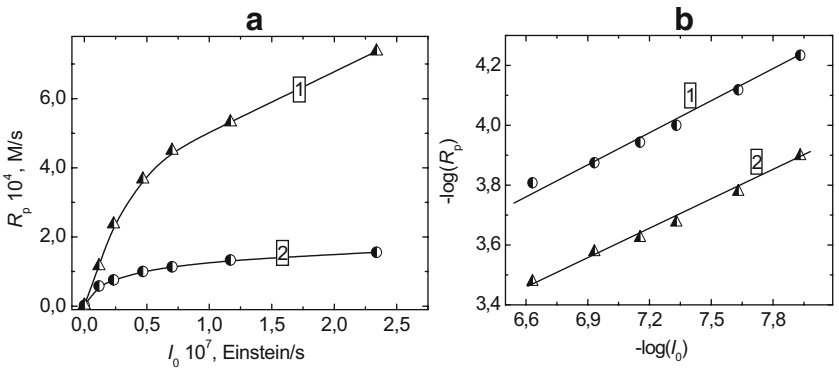

Fig. 8 **a** The rate of AAc (*curve 1*) and AAm (*curve 2*) photopolymerization vs irradiated light intensity I_0. For the *curve 1*: [AAc]=1.0 M, [CdS]=1×10^{-3} M, [SPP]=3×10^{-3} M, degassed solution. For the *curve 2*: [AAm]=0.5 M, $[Cd_{0.5}Zn_{0.5}S]=1\times10^{-3}$ M, [SPP]=3×10^{-3} M, air-exposed solution. **b** Linearization of *curves 1* and *2* in the logarithmic coordinates

Table 2 Quantum yield (Φ) of the AAc photopolymerization in the presence of CdS NPs

Number	[CdS] $\times 10^3$, M	[AAc], M	$I_0 \times 10^7$, Einstein$\times s^{-1}$	Φ
1	0	0.5	1.52	0
	0.5			2.0
	1.0			3.6
	2.0			4.3
2	1.0	0.2		0.6
		0.4		1.4
		0.6		2.6
		0.8		4.0
		1.0		5.7
3[a]		1.0	0.12	25.8
			0.23	20.6
			0.47	16.0
			0.70	11.8
			1.17	9.3
			2.34	6.4

[a] In degassed solution, in other cases—in air-exposed solutions

From the Eq. 26, the quantum yield of the photoinitiation β can be calculated. Table 1 presents the β values calculated for the AAm photopolymerization in the presence of various $Cd_xZn_{1-x}S$ NPs using the well-known constant $k_p/k_t^{0.5}=4.7$ (20 °C [33]). The quantum yields of the photoinitiation are quite small and fall in the range 10^{-4}–10^{-3}.

Table 3 The quantum yields (Φ) of acrylamide photopolymerization in the presence of $Cd_{0.5}Zn_{0.5}S$ NPs

Number	$[Cd_{0.5}Zn_{0.5}S]\times 10^3$, M	[AAm], M	$I_0 \times 10^7$, Einstein$\times s^{-1}$	O_2 presence	Φ
1	0	0.5	1.67	+	–
	0.25				1.4
	0.5				4.4
	1.0				4.6
				–	5.4
			2.34		3.8
					4.4[(1)]
					0.9[(2)]
2		0.2	1.67	+	1.6
		0.4			3.2
		0.6			5.8
		0.8			8.6
		1.0			11.4
3		0.5	0.12		11.2
			0.23		7.7
			0.47		4.9
			0.70		3.8
			2.34		1.6

[a] In the presence of 0.1 M Na_2SO_3
[b] In the presence of 1×10^{-3} M MV^{2+}

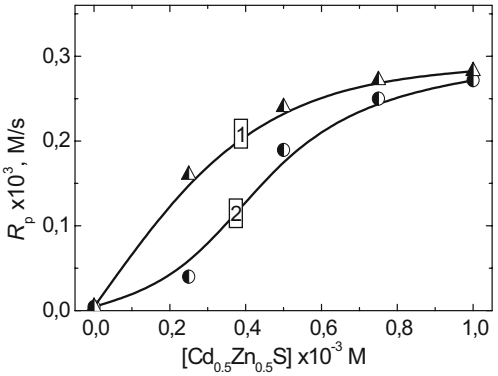

Fig. 9 The rate of $Cd_{0.5}Zn_{0.5}S$ NPs-initiated AAm photopolymerization in degassed solution (*1*) and in the presence of air (*2*) vs $Cd_{0.5}Zn_{0.5}S$ concentration. [AAm]=0.5 M, $I_0=1.67\times10^{-7}$ Einstein/s

An additional method for the evaluation of the quantum yields of the photoinitiation of acrylic monomers polymerization in the presence of semiconductor NPs in alcoholic media was proposed in [7]. According to this approach β is assumed equal to the quantum yield of the photocatalytic reduction of methylviologen ($\Phi(MV^{\bullet+})$). There is good agreement between β and $\Phi(MV^{\bullet+})$ obtained for the $Cd_xZn_{1-x}S$ NPs of different composition which suggests that the method is also suitable for the evaluation of the photoinitiation efficiency in aqueous media studied in the present work.

Conclusions

The principal results of the present work can be summarized as follows.

Photocatalytic activity of CdS and $Cd_xZn_{1-x}S$ NPs in the polymerization of acrylic acid and acrylamide in aqueous solutions was found. The dominant pathway of the generation of primary radicals was suggested to be the reduction of adsorbed monomers by the conduction band electrons of $Cd_xZn_{1-x}S$ nanoparticles. Two complimentary photoinitiation channels were assumed to exist—the monomer oxidation by the valence band holes and the addition of photocatalytically produced hydrogen to monomer molecules.

A correlation between the composition of $Cd_xZn_{1-x}S$ nanoparticles and their photocatalytic activity in the polymerization of acrylamide was found. Growth of the conduction band potential of the semiconductor nanoparticles at an increase in the molar Zn^{II} fraction was suggested as the main reason for the growth of the quantum efficiency of the photocatalytic polymerization.

An expression for the rate of the photocatalytic polymerization was deduced from which the quantum yields of the photoinitiation were evaluated to be as small as 10^{-4}–10^{-3}.

References

1. Henglein A (1984) Pure Appl Chem 56:1215
2. Kryukov AI, Kuchmiy SY, Pokhodenko VD (2000) Theor Exp Chem 36:63
3. Roy AM, De GC (2003) J Photochem Photobiol A Chem 157:87
4. Zeug N, Bücheler J, Kisch H (1985) J Am Chem Soc 107:1459
5. Kobayashi K, Kitaguchi K, Tanaka H et al (1987) J Chem Soc, Faraday Trans 1 83:1395
6. Ueno A, Kakuta N, Park KH et al (1985) J Phys Chem 89:3828
7. Hoffman AJ, Lee H, MIlls G, Hoffmann MR (1992) J Phys Chem 96:5540
8. Hoffman AJ, Lee H, MIlls G, Hoffmann MR (1992) J Phys Chem 96:5546
9. Dong C, Ni X (2004) J Macromol Sci A41:547
10. Stroyuk AL, Granchak VM, Korzhak AV, Kuchmiy SY (2004) J Photochem Photobiol A Chem 162:339
11. Ojah R, Dolui SK (2006) Sol Energy Mater Sol Cells 90:1615
12. Ojah R, Dolui SK (2005) J Photochem Photobiol A Chem 172:121
13. Kuriacose JC, Markham MC (1961) J Phys Chem 65:2232
14. Kraeutler B, Reiche H, Bard AJ (1979) J Polym Sci Polym Lett Ed 17:535
15. Kamat PV, Todesco RV (1987) J Polym Sci, A: Polym Chem 25:1035
16. Huang ZY, Barber T, Mills G, Morris MB (1994) J Phys Chem 98:12746
17. Kryukov AI, Sherstyuk VP, Dilung II (1982) The photoinduced electron transfer and its applications. Naukova dumka, Kyiv
18. Liska R, Schwager F, Maier C, Cano-Vives R, Stampfl J (2005) J Appl Polymer Sci 97:2286
19. Davidenko N, Garcia O, Sastre R (2003) J Biomater Sci Polymer Ed 14:733
20. Raevskaya AE, Stroyuk AL, Kryukov AI, Kuchmiy SY (2006) Theor Exp Chem 42:181
21. Raevskaya AE, Stroyuk AL, Kuchmiy SY (2003) Theor Exp Chem 39:158
22. Raevskaya AE, Stroyuk AL, Kuchmiy SY (2004) J Nanopart Res 6:149
23. M. Grätzel (ed) (1986) Energy resources through photochemistry and catalysis. Academic, New York
24. Gaponenko SV (1996) Optical properties of semiconductor nanocrystals. University Press, Cambridge
25. Zhang JZ (2000) J Phys Chem B 104:7239
26. Zhang JZ, O'Neil RH, Roberti TW (1994) J Phys Chem 98:3859
27. Albery JW, Brown GT, Darwent JR, Saievar-Iranizad E (1985) J Chem Soc, Faraday Trans 1 81:1999
28. Bavykin DV, Savinov EN, Parmon VN (2000) J Photochem Photobiol A Chem 130:57
29. Kamat PV, Dimitrijevič NM, Nozik AJ (1989) J Phys Chem 93:2873
30. Matsumoto H, Uchida H, Matsunaga T, Tanaka K et al (1994) J Phys Chem 98:11549
31. Bamford CH, Barb WG, Jenkins AD, Onyon PF (eds) (1958) The kinetics of vinyl monomers polymerization by radical mechanisms. Butterworths Scientific Publications, London
32. George MH, Ghosh A (1978) J Polym Sci Polym Chem Ed 16:981
33. Bagdasaryan HS (1966) Theory of radical polymerization. Nauka, Moscow
34. Goronovski IT, Nazarenko YP, Nekryatch EF (1974) Handbook of chemistry. Naukova dumka, Kyiv
35. Terenin AN (1967) The photonics of dyes and related compounds. Nauka, Leningrad
36. Kamat PV, Dimitrijevič NM, Fessenden RW (1987) J Phys Chem 91:396
37. Nosaka Y, Fox MA (1986) J Phys Chem 90:6521